Second-order Monte Carlo wave-function approach to the relaxation effects on ringing revivals in a molecular system interacting with a strongly squeezed coherent field

Masayoshi Nakano,* Ryohei Kishi, and Tomoshige Nitta

Division of Chemical Engineering, Department of Materials Engineering Science, Graduate School of Engineering Science, Osaka University, Toyonaka, Osaka 560-0043, Japan

Kizashi Yamaguchi

Department of Chemistry, Graduate School of Science, Osaka University, Toyonaka, Osaka 560-0043, Japan

We investigate the relaxation effects on the quantum dynamics in a two-state molecular system interacting with a single-mode strongly amplitude-squeezed coherent field using the second-order Monte Carlo wave-function method. The molecular population inversion (collapse-revival behavior of Rabi oscillations) is known to show the echoes after each revival, which are referred to as ringing revivals, in the case of strongly squeezed coherent fields with oscillatory photon-number distributions due to the phase-space interference effect. Two types of relaxation effects, i.e., cavity relaxation (the dissipation of an internal single mode to outer mode) and molecular coherent (phase) relaxation caused by nuclear vibrations on ringing revivals are investigated from the viewpoint of the quantum-phase dynamics using the quasiprobability (Q function) distribution of a single-mode field and the off-diagonal molecular density matrix $|\rho_{\text{elec } 1,2}(t)|$. It turns out that the molecular phase relaxation attenuates both the entire revival-collapse behavior and the increase in $|\rho_{\text{elec } 1,2}(t)|$ during the quiescent region, whereas a very slight cavity relaxation particularly suppresses the echoes in ringing revivals more significantly than the first revival but hardly changes a primary variation in envelope of $|\rho_{\text{elec } 1,2}(t)|$ in the nonrelaxation case.

I. INTRODUCTION

It is well known that the interaction among quantized photon fields with various statistics and atomic systems causes lots of attractive dynamical quantum behavior, e.g., collapse and revival, of atomic/molecular population inversion [1–19]. The mechanism and the features of collapse and revival behaviors have been well analyzed [6–13]: these two behaviors are found to originate in the dephasing and the rephasing among Rabi oscillations with slight different frequencies, respectively. A peculiar collapse-revival behavior appears in the ringing revivals of a single two-state atom interacting with a strongly squeezed coherent field with oscillatory photon-number distributions [20]. In this behavior, the collapse following revival exhibits oscillatory echoes, which are predicted to be caused by the two origins: the distinct photon-number distribution peaks with different rephasing times and the interference among the different peaks, exhibiting distinct echoes rather than a blurred extended collapse of the primary revival.

In general, the interaction between an atomic/molecular system and a quantized photon field is known to be significantly influenced by various relaxation effects, strongly suppressing the collapse-revival behavior [21–27]. In our previous paper [28], we have examined the quantum-phase dynamics composed of a weakly amplitude-squeezed coherent field [29–36] and a two-state molecular model in order to elucidate the cavity relaxation (the dissipation of cavity mode to outer mode through walls or mirrors) and the mo-

lecular phase relaxation (caused by the nuclear vibrations) effects on the collapse-revival behaviors. These relaxations have been shown to cause a significant suppression of not only the collapse-revival behavior of molecular population but also the coherency (entanglement) between the molecular electronic states. This result therefore suggests remarkable relaxation effects on the ringing revivals in the case of strongly squeezed coherent field.

We employ, in this study, the Jaynes-Cummings model [1] composed of a two-state atom/molecule interacting with a single-mode strongly amplitude-squeezed coherent field. The quantum master equation [37] is derived for this system and the Monte Carlo wave-function (MCWF) method [38–42] is applied in order to treat a large number of photon-number bases for the strongly squeezed coherent field. In the MCWF method, the dynamics is described by a Schrödinger-like wave equation with non-Hermitian Hamiltonian, though the quantum jumps randomly interrupting the coherent motion of the system have to be introduced. As a result, the MCWF method generates a large number of independent quantum trajectories of wave functions. This point provides an advantage of the MCWF method since the numerical effort in the direct integration of the quantum master equation using the reduced density matrices is proportional to N^2, which denotes the respective state space, while that for the MCWF method (which treats only the effective wave function) is proportional to N. Although the first-order unraveling (Euler) method is usually employed in the MCWF method, in the present study, a more efficient second-order unraveling method is applied according to the method developed by Steinbach *et al.* [43]. In order to clarify the effects of these relaxations on the ringing revivals, the molecular coherency

*Email address: mnaka@cheng.es.osaka-u.ac.jp

and photon phase dynamics are examined, as well as molecular and photon field population dynamics, using the dynamical behavior of quasiprobability (Q function) distribution [21,22] of cavity photon field and off-diagonal molecular density matrices [44–53], which represent a coherency between molecular electronic states.

Although the cavity relaxation effects have been studied for atomic systems coupled with quantized coherent fields, there have been few studies on the effects of cavity relaxation and pure-phase relaxation, caused by molecular vibration and atom-phonon interaction, on the quantum phase dynamics, in particular, the ringing revival behavior, of molecules and/or atomic clusters interacting with strongly squeezed coherent fields. The present study therefore first contributes to the understanding of such interaction dynamics though there are not still practical realizations by experiments for our theoretical and computational predictions. Such study will become important from the viewpoint of realization of novel control of electronic coherency, which will be applied to quantum-information devices, e.g., quantum computer. Also as an attempt of interdisciplinary study between quantum optics and chemistry, the present study is characterized by two aspects: the relaxation effects, which are seriously important for applying to the molecular systems, and the application of the high-order MCWF method, which is also essential for treating actual molecular systems with a large number of freedoms.

This paper is organized as follows. In Sec. II, we show a molecule-photon coupled model (Sec. II A), the second-order MCWF method (Sec. II B) as well as explicit forms of relaxation operators for this model (Sec. II C). The relaxation effects on the ringing revivals of molecular population (diagonal molecular density matrix) and the average photon number are investigated in Sec. III A. In Sec. III B, the dynamical behaviors of off-diagonal molecular density matrix and Q function distributions of cavity field are examined to analyze the effects of relaxations on the quantum-phase properties of ringing revivals. These results are summarized in Sec. IV.

II. METHODOLOGY

A. Molecule-photon coupling, system-reservoir coupling, and a strongly squeezed cavity field

Figure 1 shows a calculated model composed of a molecular electronic-state model, nuclear vibrations, a single-mode strongly amplitude-squeezed photon field (cavity field), and an external field (outside a cavity). We regard the molecular electronic-state model and a cavity field as a "system" that we focus on, while do the nuclear vibrations (phonon bath) and an external field (thermal photon bath) as two types of "reservoirs" with an infinite number of bosons.

The Hamiltonian of a system H_S is expressed by

$$H_S = H_{elec} + H_{cfield} + H_{elec-cfield}, \qquad (1)$$

where H_{elec}, H_{cfield}, and $H_{elec-cfield}$ represent Hamiltonians for a two-state molecular model, a cavity field, and an interaction between them, respectively. The explicit forms of these Hamiltonians are given by
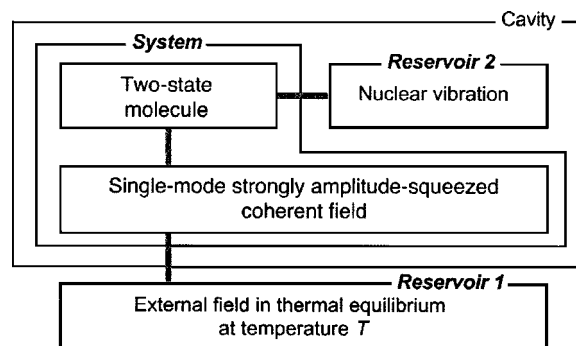
FIG. 1. System composed of a two-state electronic state of a molecule coupled with a single-mode photon field in a cavity and a reservoir composed of nuclear vibrations and an external field in thermal equilibrium at temperature T. We consider a two-state molecular model (with transition energy $E_{21} = 20\,000$ cm^{-1}, and transition moment $\mu_{21} = 15$ D) coupled with an strongly amplitude-squeezed field [$\phi = 0$ and $r = 1.5$, see Eq. (8)]. This field has an initial average photon number $\langle \hat{n} \rangle = 16$ and a frequency $\omega = 20\,000$ cm^{-1}) in a cavity with $V = 10^7$ Å^3 surrounded by outer-mode reservoir with $T = 300$ K.

$$H_{elec} = \sum_i^2 E_i a_i^\dagger a_i, \qquad (2)$$

$$H_{cfield} = \left(b^\dagger b + \frac{1}{2} \right) \omega, \qquad (3)$$

and

$$H_{elec-cfield} = \sum_{i,j}^2 K d_{ij} a_i^\dagger a_j (b^\dagger + b), \qquad (4)$$

where

$$K = \left(\frac{2\pi\omega}{V} \right)^{1/2}. \qquad (5)$$

In Eq. (2), E_i indicates the energy of the molecular electronic state i, $a_i^\dagger$, and a_i are, respectively, the creation and annihilation operators for the quantized electron field in the ith electronic energy state. In Eq. (3), $b^\dagger$ and b are the creation and annihilation operators for the single-mode photon field with a frequency ω. In Eq. (4), d_{ij} is the matrix element of the molecular electronic dipole moment operator in the direction of the polarization of a single-mode photon field. In Eq. (5), V is the volume of a cavity containing the single-mode photon field.

We here consider two types of reservoirs composed of an ensemble of harmonic oscillators, photons (R$_1$, an external field) and phonons (R$_2$, nuclear vibrations), respectively. The interaction between cavity field and R$_1$ and that between electronic states and R$_2$ are described, respectively, by the Hamiltonians

$$H_{cfield-R_1} = \sum_j (\xi_j^* b r_{1j}^\dagger + \xi_j b^\dagger r_{1j}) \qquad (6)$$

and

$$H_{\text{elec}-R_2} = \sum_{i,j} \gamma_{ij} a_j^\dagger a_j (r_{2i} + r_{2i}^\dagger), \tag{7}$$

where $r_{1j}^\dagger$ and r_{1j} represent the photon creation and annihilation operators of reservoir 1 (external field), and $r_{2i}^\dagger$ and r_{2i} represent the phonon creation and annihilation operators of reservoir 2 (nuclear vibrations), respectively. The ξ_j and γ_{ij} indicate the coupling constant between a cavity field and an external field and that between electrons and vibrational phonons, respectively.

The squeezed coherent field is generated by various non-linear optical processes including optical parametric oscillation and four-wave mixing [29–36]. Theoretically, the single-mode ideally squeezed coherent field can be generated from the vacuum field $|0\rangle$ by operating squeezing and displacement operators [29–35]:

$$|\beta, \zeta\rangle = \exp(\beta b^\dagger - \beta^* b) \exp[(\zeta^* b^2 - \zeta b^{\dagger 2})/2]|0\rangle, \tag{8}$$

where ζ can be expressed by $\zeta = re^{i\phi}$ using real modulus r and argument ϕ. The r and $\phi/2$ represent squeezing intensity and direction, respectively. The direction of β is taken to be aligned with $\text{Re}(\beta)$ axis in the complex β plane. In this field, the variance of the quadrature operator $\hat{x}_1(\hat{x}_2)$ can be less than the value 1/2 for the vacuum and the coherent field states. From the Heisenberg uncertainty relation between $\hat{x}_1$ and $\hat{x}_2$, the variance of another quadrature operator $\hat{x}_2(\hat{x}_1)$ exceeds 1/2. If $\phi=0$ in Eq. (8) with a relatively small squeezing intensity r, the squeezed coherent field has larger phase uncertainty than a coherent field with the same average photon number and exhibits a narrower (sub-Poissonian) photon-number distribution. Such field is referred to as an amplitude-squeezed coherent field. The elements of the squeezed field density matrix are represented by [29–35]

$$\rho_{\text{photon } n,m}(t_0) = \frac{1}{|\mu|\sqrt{n!\,m!}} \left(\frac{\nu}{2\mu}\right)^{n/2} \left(\frac{\nu^*}{2\mu^*}\right)^{m/2} \exp(-|\beta'|^2)$$

$$\times \exp\left(\frac{1}{2}\frac{\nu^*}{\mu}\beta'^2 + \frac{1}{2}\frac{\nu}{\mu^*}\beta'^2\right) H_m^*\left(\frac{\beta'}{\sqrt{2\mu\nu}}\right)$$

$$\times H_n^*\left(\frac{\beta'}{\sqrt{2\mu\nu}}\right), \tag{9}$$

where $\mu = \cosh r$, $\nu = e^{i\phi}\sinh r$, $\beta' = \mu\beta + \nu\beta^*$, and H_n is Hermite function. The diagonal part of Eq. (9) indicates the photon-number distribution of squeezed coherent field. Satyanarayana *et al.* [20] designate the amplitude-squeezed coherent fields as strongly squeezed coherent fields if they satisfy the condition: $\exp(2r) \geq |\beta|^{2/3}$, where the variance in photon number originating in the squeezing part matches the contribution originating in coherent field part. The strongly squeezed coherent field is characterized by the feature that its photon-number distribution is oscillatory. Such oscillatory distribution is explained in terms of interference in the phase space [54]: the oscillatory photon distribution is caused by the interference between contribution from two regions in phase space where an elongated ellipse [see the Q function shown in Fig. 5(I)] overlaps the annuli indicating the number states.
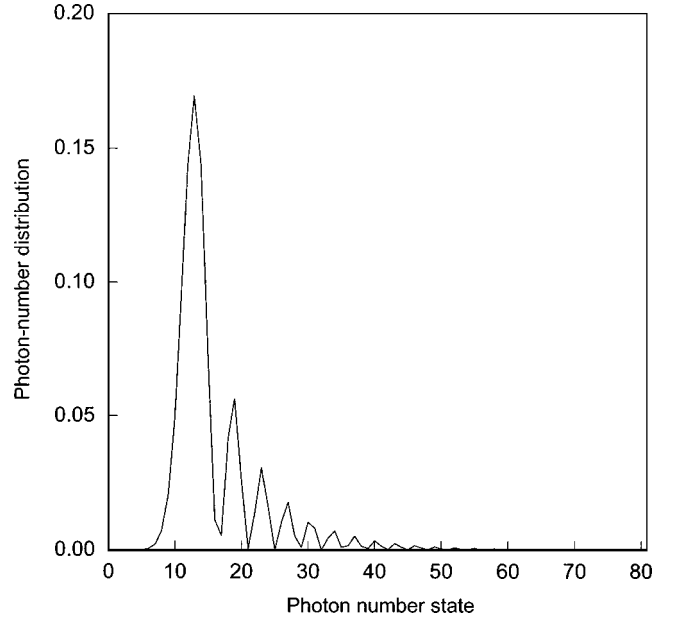
FIG. 2. Photon-number distributions for a strongly amplitude-squeezed field.

We consider a two-state molecular model with an energy interval $E_{21}(\equiv E_2 - E_1) = 20\ 000\ \text{cm}^{-1}$ and a transition moment $d_{21} = 15$ D along the polarization of cavity field. The cavity volume V [Eq. (5)] is assumed to be 10^7 Å^3. The averaged photon number and the squeezing intensity of the initial strongly amplitude-squeezed field are fixed to $\langle \hat{n} \rangle = 16$ and $r = 1.5$, respectively. These values satisfy the above condition: $\exp(2r)/|\beta|^{2/3} \approx 8.907 > 1$. Figure 2 shows the oscillatory photon-number distribution for this strongly amplitude-squeezed coherent field. It is noted that the distribution is super-Poissonian overall, while individual peaks within this distribution are sub-Poissonian.

B. Second-order Monte Carlo wave-function method

In this section, we briefly explain our calculation scheme. The quantum master equation can be written by

$$\dot{\rho}_S = i[\rho_S, H_S] + \mathcal{L}_{\text{relax}}\rho_S, \tag{10}$$

where the Hamiltonian for the system is H_S, and $\mathcal{L}_{\text{relax}}$ indicates the relaxation superoperator, describing the system relaxation through its coupling to the reservoirs. The atomic unit ($\hbar = m_e = e = 1$) is used throughout this paper. In the Born-Markov approximation [37], the relaxation superoperator is represented by the Lindblad form [55]:

$$\mathcal{L}_{\text{relax}}\rho_S = -\frac{1}{2}\sum_m (C_m^\dagger C_m \rho_S + \rho_S C_m^\dagger C_m) + \sum_m C_m \rho_S C_m^\dagger. \tag{11}$$

This type of relaxation operator is widely applied in dissipative dynamics in quantum optics, chemical physics, biology, and so on. The Lindblad operators $C_m^\dagger$ and C_m act on the system, and their forms depend on the nature of problem.

The original MCWF method simulates the evolution of quantum trajectories in Hilbert space conditioned on continu-

ous photodetection involving two types of elements: one is smooth evolution by the non-Hermitian Hamiltonian H_{eff}, which originates in the first terms on the right-hand side of Eqs. (10) and (11), and another represents the random interruptions of the non-Hermitian evolution by projections (quantum jumps) described by the second term on the right-hand side of Eq. (11). The higher-order unravelings in the MCWF method are advantageous to obtaining more accurate and stable numerical results [28,43]. In this study, the second-order unraveling method is employed to provide a feasible approach treating a large number of photon bases. From the integration of the quantum master equation (10) to second order in δt, the following form is obtained [43]:

$$\rho_{\mathrm{S}}(t+\delta t) = U\rho_{\mathrm{S}}(t)U^{\dagger} + \frac{1}{2}\delta t \sum_{m} UC_{m}\rho_{\mathrm{S}}(t)C_{m}^{\dagger}U^{\dagger}$$

$$+\frac{1}{2}\delta t \sum_{m} C_{m}U\rho_{\mathrm{S}}(t)U^{\dagger}C_{m}^{\dagger}$$

$$+\frac{1}{2}\delta t^{2}\sum_{m,n} UC_{m}C_{n}\rho_{\mathrm{S}}(t)C_{n}^{\dagger}C_{m}^{\dagger}U^{\dagger} + O(\delta t^{3}). \tag{12}$$

Here, U indicates the non-Hermitian evolution, which is referred to as the "no-jump" evolution, under the influence of the effective Hamiltonian Eq. (14):

$$U = \exp(-iH_{\mathrm{eff}}\delta t), \tag{13}$$

where

$$H_{\mathrm{eff}} = H_{\mathrm{S}} - \frac{i}{2}\sum_{m} C_{m}^{\dagger}C_{m}. \tag{14}$$

Each term on the right-hand side of Eq. (12) represents the "minitrajectory" [43]. The density-matrix evolution can be simulated with pure states by using an expansion of the density matrix into minitrajectories. The procedure for evolving wave functions of a system is described as follows. The normalized wave function $|\Psi(t+\delta t)\rangle$ of a system (molecular electronic state + cavity single mode) and the probability δp_{l} to choose its evolution in time step δt for each minitrajectory in Eq. (12) is represented by

(m1) $|\Psi(t+\delta t)\rangle = \dfrac{U|\Psi(t)\rangle}{\sqrt{\delta p_{1}}},$

$$\delta p_{1} = \langle\Psi(t)|U^{\dagger}U|\Psi(t)\rangle, \quad \text{(no jump)}, \tag{15}$$

(m2) $|\Psi(t+\delta t)\rangle = \dfrac{UC_{m}|\Psi(t)\rangle}{\sqrt{\delta p_{2m}/(\delta t/2)}},$

$$\delta p_{2m} = \langle\Psi(t)|C_{m}^{\dagger}U^{\dagger}UC_{m}|\Psi(t)\rangle\frac{\delta t}{2}, \tag{16}$$

(m3) $|\Psi(t+\delta t)\rangle = \dfrac{C_{m}U|\Psi(t)\rangle}{\sqrt{\delta p_{3m}/(\delta t/2)}},$

$$\delta p_{3m} = \langle\Psi(t)|U^{\dagger}C_{m}^{\dagger}C_{m}U|\Psi(t)\rangle\frac{\delta t}{2}, \tag{17}$$

and

(m4) $|\Psi(t+\delta t)\rangle = \dfrac{UC_{m}C_{n}|\Psi(t)\rangle}{\sqrt{\delta p_{4m}/(\delta t^{2}/2)}},$

$$\delta p_{4mn} = \langle\Psi(t)|C_{n}^{\dagger}C_{m}^{\dagger}U^{\dagger}UC_{m}C_{n}|\Psi(t)\rangle\frac{\delta t^{2}}{2}. \tag{18}$$

Details of the numerical calculation procedure of the wave-function at time $t+\delta t$ using the Monte Carlo method are presented in Ref. [28].

After obtaining a sufficiently large number of trajectories $\rho_{\mathrm{S}}^{(i)}(t)[=|\Psi^{(i)}(t)\rangle\langle\Psi^{(i)}(t)|]$ constructed by the Monte Carlo wavefunctions $|\Psi^{(i)}(t)\rangle$, in which i indicates the trajectory number $(i=1,\ldots,M_{\mathrm{C}})$, we average their density-matrix elements at each time t using the basis of the system $\{|k,n\rangle(\equiv|k\rangle\otimes|n\rangle)\}$ spanned by the direct product of the molecular electronic state $\{|k\rangle\}(k=1,2,\ldots,N)$ and the cavity-mode photon number state $\{|n\rangle\}(n=0,1,\ldots,\infty)$:

$$\rho_{Sk,n;k',n'}(t) \equiv \langle k,n|\rho_{\mathrm{S}}(t)|k',n'\rangle \cong \frac{1}{M_{\mathrm{C}}}\sum_{i=1}^{M_{\mathrm{C}}}\langle k,n|\rho_{\mathrm{S}}^{(i)}(t)|k',n'\rangle. \tag{19}$$

The molecular electronic-state and cavity-mode photon reduced density matrices are, respectively, calculated by

$$\rho_{\mathrm{elec}\ k,k'}(t) = \sum_{n} \rho_{Sk,n;k',n}(t), \tag{20}$$

and

$$\rho_{\mathrm{photon}\ n,n'}(t) = \sum_{k} \rho_{Sk,n;k,n'}(t). \tag{21}$$

Various properties concerning molecular electronic state and cavity mode photon can be calculated using these reduced density matrices.

The Q function of a cavity photon field is defined by [37]

$$Q(\beta,t) = \frac{1}{\pi}\langle\beta|\rho_{\mathrm{photon}}(t)|\beta\rangle$$

$$= \frac{1}{\pi}\exp(-\beta^{2})\sum_{n,n'=0}\frac{\beta^{*n}\beta^{n'}}{\sqrt{n!\,n'!}}\rho_{\mathrm{photon}\ n,n'}(t), \tag{22}$$

where $|\beta\rangle$ is a coherent state, β is its complex amplitude, and n is a photon number. The Q functions in the complex plane β at the time t are useful for gaining an insight into the dynamics of the field-amplitude and -phase probability distributions for the a single-mode photon field coupled with molecular electronic state in a cavity.

C. Relaxation terms

The relaxation of a system into two types of reservoirs is described by Eq. (11) in the quantum master equation Eq.

(10). We here consider two types of relaxation terms: cavity relaxation ($\mathcal{L}_{\text{cfield-rel}}$) and molecular phase relaxation ($\mathcal{L}_{\text{phase-rel}}$). The former represents the leakage of single-mode photons from the cavity to outer modes originating in the coupling between a cavity single mode and external modes, while the latter describes the phase relaxation in a molecule caused by the coupling among molecular electronic states and nuclear vibrations. The explicit forms of these relaxation terms are given by [28]

$$\mathcal{L}_{\text{cfield-rel}}\rho_S = \frac{\gamma}{2}(2b\rho_S b^\dagger - b^\dagger b \rho_S - \rho_S b^\dagger b) + \gamma \bar{n}_R(b^\dagger \rho_S b$$

$$+ b\rho_S b^\dagger - b^+ b\rho_S - \rho_S bb^\dagger) \tag{23}$$

and

$$\mathcal{L}_{\text{phase-rel}}\rho_S = - \sum_{i,j(i\neq j)} \Gamma'_{ji} P_{jj}\rho_S P_{ii}, \tag{24}$$

where P_{ij} is a projection operator concerning molecular electronic states:

$$P_{ij} = |i\rangle\langle j|. \tag{25}$$

In Eq. (23), γ indicates the relaxation rate of the cavity mode, and $\bar{n}_R$ stands for the average photon number in thermal equilibrium at temperature T at the cavity-mode frequency ω:

$$\bar{n}_R = \left[\exp\left(\frac{\omega}{k_B T}\right) - 1\right]^{-1}, \tag{26}$$

where k_B is the Boltzmann's constant. The phase relaxation (the relaxation of off-diagonal molecular density matrices) in Eq. (24) is described by a phase relaxation rate $\Gamma'_{ij}(=\Gamma'_{ji})$. It is noted that these relaxation rates, γ and Γ'_{ij}, are functions of system-reservoir coupling constants, ξ_j and γ_{ij}, respectively [57].

Using Eqs. (23) and (24), the explicit forms of Lindblad operators C_m in Eq. (11) in the second-order MCWF method are described as follows. For the cavity relaxation [Eq. (23)], we have to deal with the following two operators [41]:

$$C_1 = [\gamma(1 + \bar{n}_R)]^{1/2}b \tag{27}$$

and

$$C_2 = [\gamma\bar{n}_R]^{1/2}b^\dagger, \tag{28}$$

which describe the quantum jumps corresponding to a dissipation by a spontaneous or a stimulated emission and an excitation by the absorption of a reservoir photon at temperature T, respectively. The Lindblad operators for the dephasing part [Eq. (24)] are expressed by [56]

$$C_n = \sqrt{\frac{\Gamma''_{ij}}{2}}(P_{jj} - P_{ii}), \quad (_N C_2 + 2 \geq n \geq 3), \tag{29}$$

where N represents the number of molecular electronic states, and n corresponds to a pair of states $(i,j)(i<j)$. The new factor Γ''_{ij} is related to the dephasing rate Γ'_{kl} as

$$\Gamma'_{kl} = \frac{1}{4}\left(\sum_{i(\neq k)} \Gamma''_{ik} + \sum_{i(\neq l)} \Gamma''_{il}\right) + \frac{1}{2}\Gamma''_{kl}. \tag{30}$$

III. RESULTS AND DISCUSSION

A. Dynamics of molecular population and average photon number

At the initial time, the molecule is assumed to be in the ground state and not to be coupled with the strongly amplitude-squeezed field (see Sec. II A). In a numerical calculation, the size of a photon-number basis is fixed to be 81, which is found to be sufficient for our study. The effects of two types of relaxations, (i) cavity relaxation and (ii) molecular phase relaxation are examined as well as the nonrelaxation case. The cavity relaxation rate is $\gamma = 0.5$ cm^{-1} [see Eq. (23)] and the molecular phase relaxation rate is $\Gamma'_{21} = 10$ cm^{-1} [see Eqs. (24)]. The temperature of the outer mode reservoir is fixed to be 300 K. It is well known that the sample size M_C of Monte Carlo trajectories and time step δt have a significant influence on the numerical error of the results. In the non-Hermitian evolution [Eq. (13)], we employ the sixth-order Runge-Kutta method with the time step, $\delta t \approx 0.0345$ a.u. (a period of a cavity field/2000), which is found to provide a sufficiently converged and quantitatively correct results for a dynamical behavior of molecular population and average photon number for the nonrelaxation model. The numerical error for the relaxation case also originates in the Monte Carlo method, in which the error is found to be proportional to $1/\sqrt{M_C}$ [43]. We have checked the convergence behaviors of molecular ground-state population and average photon numbers for a model system with relaxations and have found that $M_C = 10\,000$ can provide qualitatively converged behavior.

Figure 3 shows the variation in the ground-state molecular population for a nonrelaxation (a), cavity relaxation (b), and molecular phase relaxation (c) cases. In the nonrelaxation case (a), similarly to the previous study [20], the revivals after the first collapse [(I)–(III)] exhibit ringing behavior: a large revival [(IV)] followed by a series of echoes [after (IV)] in contrast to the initial coherent field case, which exhibits a simple collapse envelope. Such ringing revivals are found to be caused by the fact that the different peaks in photon-number distribution (Fig. 2) give different rephasing times for the cosines $\cos(2\lambda t\sqrt{n})$ (λ: atom/molecule-field coupling constant, and n: photon number), and also each echo is not independent but interferes with each other in phase space, leading to the distinct echoes rather than a blurred, extended collapse of the primary revival [20]. In the cavity relaxation case (b), the revival amplitudes are shown to be much reduced (about 70% reduction for the maximum revival amplitude) than those in the nonrelaxation case (a) though the cavity relaxation rate $\gamma = 0.5$ cm^{-1} is very slight. This remarkable attenuation of revival is also observed for the initial coherent field and the initial weak amplitude-squeezed field cases [28]. It is shown that the molecular phase relaxation (c) with larger relaxation rate $\Gamma'_{21} = 10$ cm^{-1} gives a similar reduction of the primary revival amplitudes [(IV)] to that in the cavity relaxation case (a), while the echoes [after (IV)] exhibit more distinct behavior than that in the cavity relaxation case (b): the ratio of revival amplitudes (VI)/(IV)≈0.1 in case (b), while 0.23 in case (c).

For the variation in average photon numbers shown in Fig. 4, the nonrelaxation case (a) shows the collapse-revival
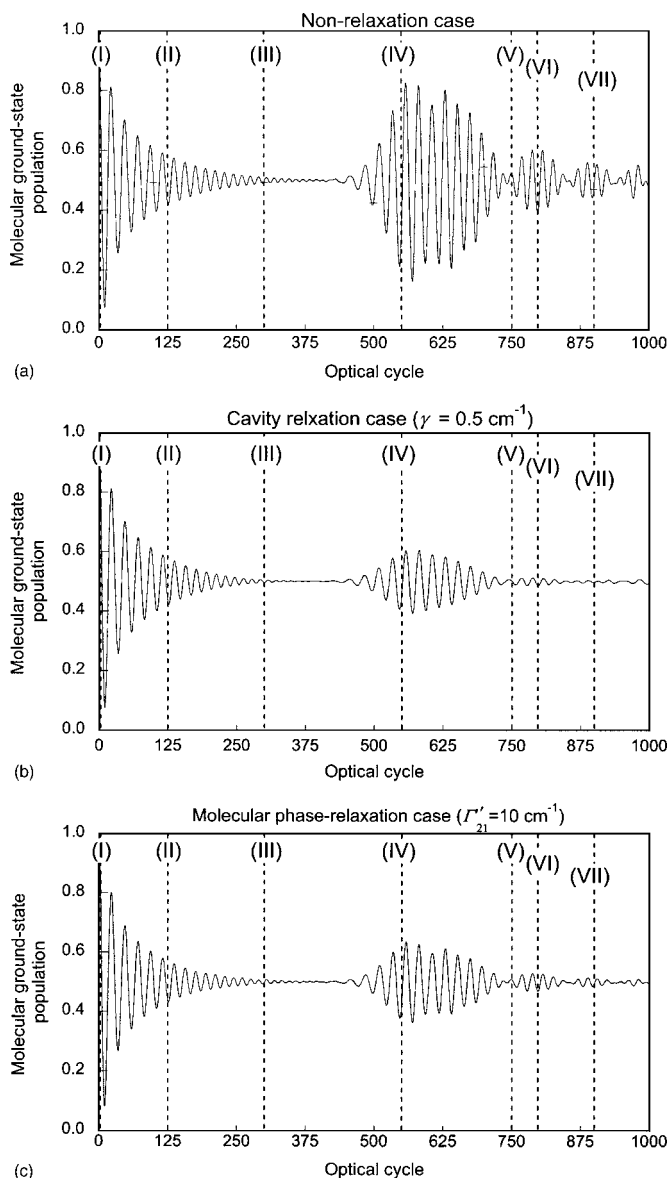
FIG. 3. Time evolutions of the molecular ground-state populations $[\rho_{\text{elec }1,1}(t)]$ for a model (Fig. 1) in the case of (a) nonrelaxation, (b) cavity relaxation ($\gamma=0.5$ cm^{-1}), and (c) molecular phase relaxation ($\Gamma'_{21}=10$ cm^{-1}). One optical cycle corresponds to $T=2\pi/\omega\approx69.0$ a.u.

behaviors involving ringing revival between $\langle n\rangle=16$ and 15 similarly to the molecular population dynamics in the nonrelaxation case [Fig. 3(a)]. The cavity relaxation case [Fig. 4(b)] shows a decrease of the average photon number as well as the significant reduction of revival-collapse amplitudes particularly in the echoes [(IV)–(VII)]. On the other hand, it turns out that the molecular phase relaxation [Fig. 4(c)] does not decay the average photon number, but only reduces the amplitudes of the revival-collapse behaviors similarly to the molecular ground-state population [Fig. 3(c)]. The features of the nondecay behaviors in the average photon number for phase relaxation can be understood by the fact that there is no energy exchange between the system and its environment by the molecular phase relaxation since the phase relaxation operators commutes with the system Hamiltonian.
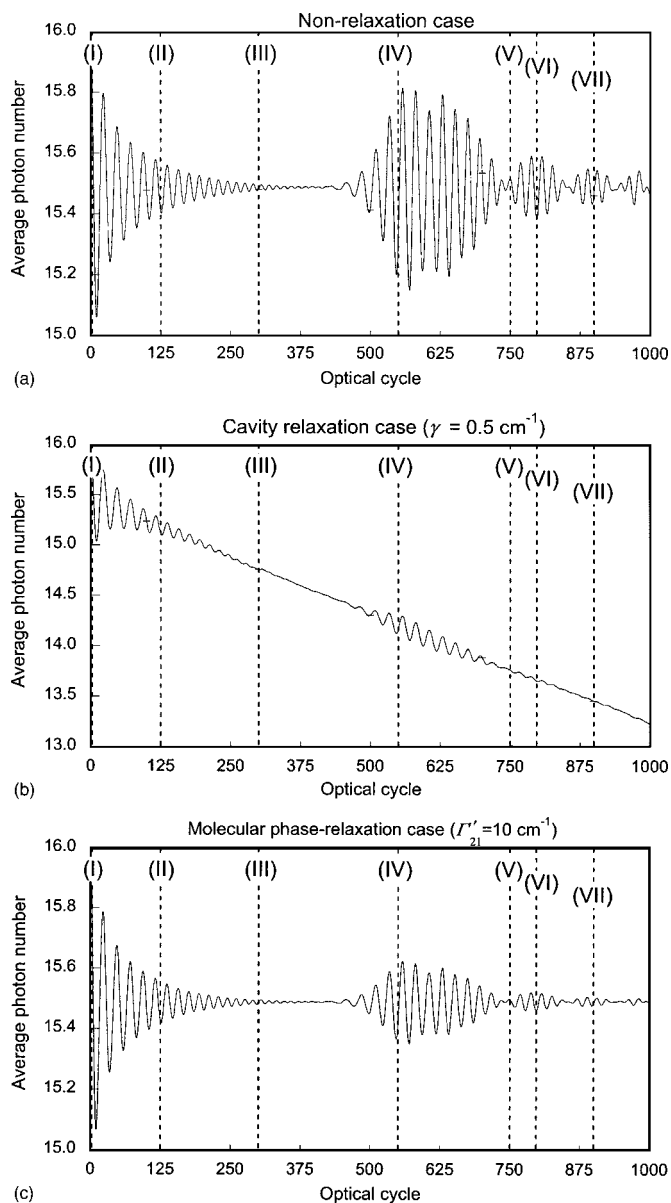
FIG. 4. Time evolutions of the average photon numbers for a model (Fig. 1) in the case of (a) nonrelaxation, (b) cavity relaxation ($\gamma=0.5$ cm^{-1}), and (c) molecular phase relaxation ($\Gamma'_{21}=10$ cm^{-1}).

B. Dynamics of quasiprobability (Q function) distributions of a cavity field

We first investigate the dynamics of Q function distributions of a cavity field in the nonrelaxation case (Fig. 5). The horizontal and perpendicular axes indicate Re(β) and Im(β), respectively. These times t are taken as $2\pi m/\omega(m=0,1,2,\ldots)$ to remove the phase (ωt) of the free field. The Q function dynamics is known to be useful for obtaining a dynamical behavior of average photon number and phase distributions for photon fields [44–53]. The initial Q function of amplitude-squeezed field is shown to provide an ellipse distribution centered around β_0 ($\equiv\sqrt{\langle\hat{n}\rangle}$, $\langle\hat{n}\rangle=16$) [see Fig. 5(I)]. The dotted circle corresponds to the average photon number $\langle\hat{n}\rangle=16$. A single peak at $\phi=0$ is found to split into two peaks and then counterrotate on the circle $|\beta|=\beta_0$ until
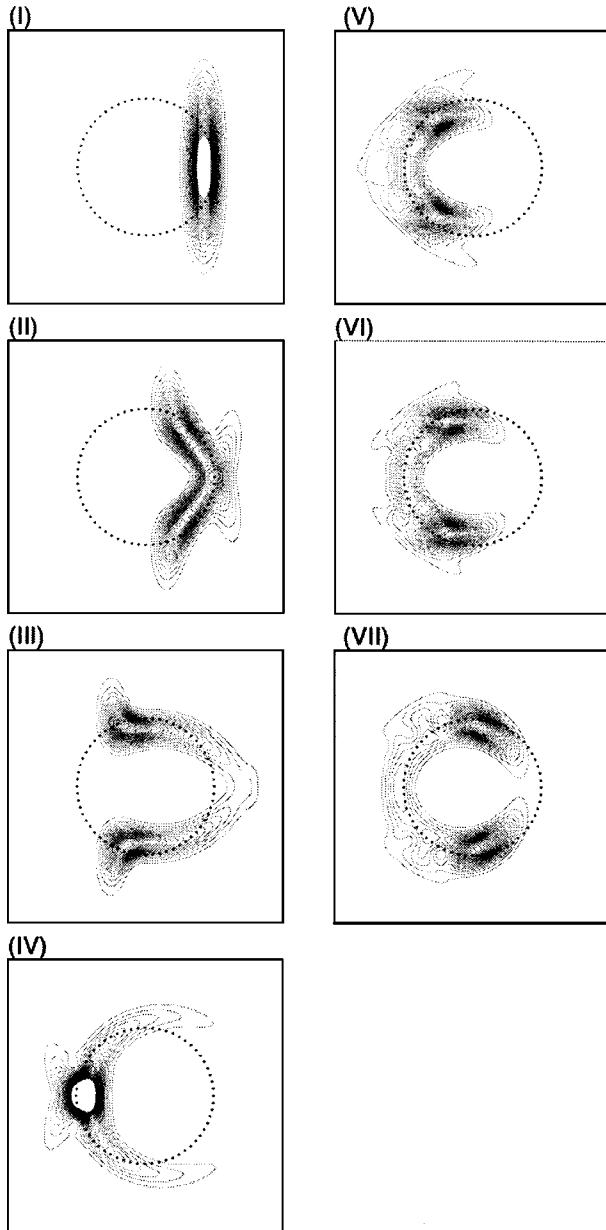
FIG. 5. Q function distributions of the amplitude-squeezed field in a cavity at times (I)–(VII) (see Figs. 3 and 4) for a coupled model (Fig. 1) in the case of nonrelaxation. The horizontal and vertical axes represent the real and imaginary parts of β, which is an eigenvalue of annihilation operator b for a cavity mode. The dotted circle with a radius $|\beta|=4$ represents the photon number 16. The 30 contours are drawn from values 0.0 to 1.0.

they collide at $\phi=\pm\pi$. After this collision, they split again and collide at $\phi=0$. These splitting and colliding processes are known to repeat though such behavior gradually gets blurred due to the number-phase uncertainty principle [21]. In contrast to the coherent field and weakly squeezed field cases [44–53], plural smaller Q function distribution peaks with different periods appear after the collision at $\phi=\pm\pi$ [(IV)]. These smaller distributions are predicted to be caused by the oscillatory photon-number distribution peaks with a different rotating speed in Q function [21]. Actually, the largest revival around (IV) corresponds to a single sharp peak at

$\phi=\pm\pi$ [Fig. 5(IV)] and its splitting does to the collapse of the largest revival, while the collision of smaller peaks with longer periods at $\phi=\pm\pi$ [Figs. 5(VI) and (VII)] correspond to the echoes of revivals at (VI) and (VII) shown in Fig. 3(a). This feature corresponds to the fact that the photon states with a large number of photons require the longer times for changing the photon phase through the interaction with a molecule [20]. It is also found that in the quiescent region [see Fig. 3(III)], the primary split peaks on the complex plane are located at $\phi=+\pi/2$ and $-\pi/2$ [Fig. 5(III)], respectively, similarly to the coherent field case, the feature of which implies the decoupling between molecule and photon field in the quiescent region, leading to the generation of an optical Schrödinger cat state [5].

We second examine the relaxation effects on the Q function distribution dynamics. Figure 6 shows the Q function distributions for the cavity relaxation case ($\gamma=0.5$ cm^{-1}). It turns out that there are almost no differences between nonrelaxation case (Fig. 5) and cavity relaxation case (Fig. 6) until (III), while the gradual decrease of the distribution in the cavity relaxation case appears particularly in the outer regions corresponding to the components with larger photon numbers [see Figs. 5(IV)–(VII) and 6(IV)–(VII)]. This can be understood by the fact that the components with a larger number of photons more significantly suffer from the cavity relaxation, whose rate is in proportion to $n\gamma$ (n: photon number) [see Eqs. (27) and (28)]. As a result, the smaller Q function distribution peaks originating in the oscillatory photon-number distribution peaks with larger numbers are shown to be reduced and thus are predicted to cause the attenuation of the revival amplitudes particularly in the echoes [see Fig. 3(b)]. On the other hand, the molecular phase relaxation ($\Gamma'_{21}=10$ cm^{-1}) is shown to remarkably blur the phase distributions, the feature of which is represented by the delocalized distributions along the dotted circle [see Fig. 7(III)–(VII)]. Such increase in the photon-phase uncertainty leads to the suppression of the amplitudes for the entire ringing revivals [see Fig. 3(c)].

C. Dynamics of off-diagonal molecular density matrix

The magnitudes of off-diagonal molecular density matrices $|\rho_{\text{elec }1,2}(t)|$ are shown in Fig. 8 in the case of nonrelaxation (a), cavity relaxation (b), and molecular phase relaxation (c). The $|\rho_{\text{elec }1,2}(t)|$ represents the degree of coherency between the ground and the excited molecular electronic states. For all the cases, the splitting and approaching to $\phi=\pm\pi/2$ of Q function [(I)–(III) shown in Figs. 5–7 correspond to the oscillatory increase in $|\rho_{\text{elec }1,2}(t)|$, at the maximum point of which the cavity-mode photon field is in a Schrödinger cat state composed of the entanglement of two phase states ($\phi=\pm\pi/2$) in the nonrelaxation case. The successive decrease in the amplitudes of $|\rho_{\text{elec }1,2}(t)|$ corresponds to the colliding process of the Q function distribution [(III)–(IV) shown in Figs. 5–7]. The split of the primary Q function distribution peak and subsequent approach to $\phi=\pm\pi/2$ [(IV)–(VII) shown in Figs. 5–7 are found to cause a gradual increase in $|\rho_{\text{elec }1,2}(t)|$ again though it accompanies the oscillations of $|\rho_{\text{elec }1,2}(t)|$ corresponding to the echoes [Fig.
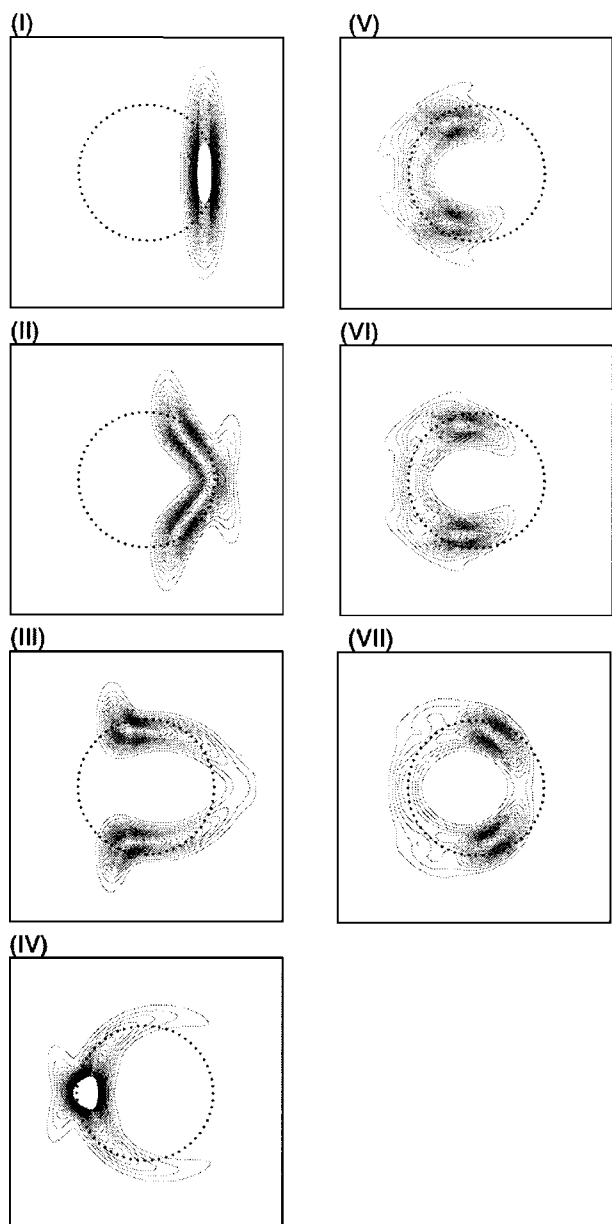
FIG. 6. Q function distributions of the amplitude-squeezed field in a cavity at times (I)–(VII) (see Figs. 3 and 4) for a coupled model (Fig. 1) in the case of cavity relaxation ($\gamma=0.7$ cm^{-1}). See Fig. 6 for further legends.

FIG. 7. Q function distributions of the amplitude-squeezed field in a cavity at times (I)–(VII) (see Figs. 3 and 4) for a coupled model (Fig. 1) in the case of molecular phase relaxation ($\Gamma'_{21}=10$ cm^{-1}).

3(a)] in the nonrelaxation case [Fig. 8(a)]. Although such primary variation in $\left|\rho_{\mathrm{elec}\ 1,2}(t)\right|$ is shown to be preserved in the case of cavity relaxation case [Fig. 8(b)] except for the oscillations in $\left|\rho_{\mathrm{elec}\ 1,2}(t)\right|$ corresponding to the echoes of revivals. In contrast to these two cases [nonrelaxation, Fig. 8(a), and cavity relaxation, Fig. 8(b) cases], the molecular phase relaxation exhibits a significant reduction (about 36%) of amplitudes of the increase in $\left|\rho_{\mathrm{elec}\ 1,2}(t)\right|$ at (III) in the nonrelaxation case. Particularly, the increase behaviors in $\left|\rho_{\mathrm{elec}\ 1,2}(t)\right|$ after (IV) in the case of nonrelaxation and cavity relaxation are shown to almost disappear in the molecular phase relaxation case [Fig. 8(c)]. This feature corresponds to the significant uncertainty of the phase distributions in Q function distributions at that time region [Fig. 7(V)–(VII)].

IV. CONCLUDING REMARKS

We have investigated the effects of two types of relaxations, i.e., cavity relaxation and molecular phase relaxation, on the dynamics of a coupled system composed of a two-state molecular model and a strongly amplitude-squeezed coherent field in a cavity using the second-order Monte Carlo wave-function (MCWF) method. In a cavity relaxation, a very slight cavity relaxation rate is found to significantly attenuate the ringing revivals, particularly the echoes. This can be understood by the fact that the Q function distributions corresponding to oscillatory photon-number distributions with larger photon numbers suffer from more signifi-
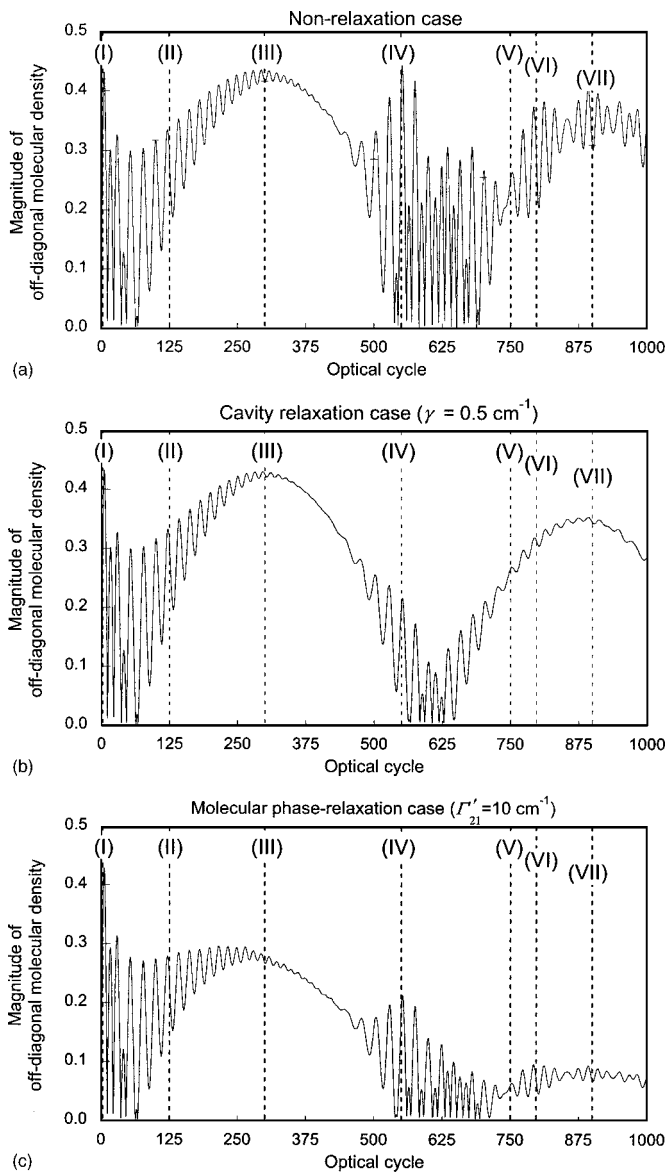
FIG. 8. Time evolutions of the magnitudes of off-diagonal molecular density matrices ($|\rho_{\text{elec } 1,2}(t)|$) for a model (Fig. 1) in the case of (a) nonrelaxation, (b) cavity relaxation ($\gamma=0.5$ cm^{-1}), and (c) molecular phase relaxation ($\Gamma'_{21}=10$ cm^{-1}).

cant cavity relaxation effects since the cavity relaxation rate is in proportion to $n\gamma$ (n: photon number). On the other hand, the primary behaviors of the degree of coherency between molecular electronic states, which is represented by the off-diagonal molecular density matrices, $|\rho_{\text{elec } 1,2}(t)|$, turn out to be preserved in the cavity relaxation case since such echoes only give the oscillations with smaller amplitudes in envelopes of $|\rho_{\text{elec } 1,2}(t)|$. In the case of molecular phase relaxation, although the entire amplitudes of ringing revivals are suppressed, the echoes appear more distinctively than those in the cavity relaxation case. The coherency between molecular electronic states, however, turns out to be more attenuated than that in the cavity relaxation case. It is predicted that this decoherency between molecular electronic states affects the photon phase properties and thus provides delocal-

ized phase distributions in Q functions, the feature of which significantly attenuates the entire ringing revivals. Judging from the present results, if the cavity relaxation could be sufficiently suppressed, the molecule coupled with a strongly amplitude-squeezed coherent field has a possibility of exhibiting ringing revivals similarly to the relaxation-free atomic case though the magnitudes of entire revival amplitudes are fairly reduced as compared to the atomic case. On the other hand, the generation of Schrödinger cat state in the quiescent region is predicted to be more significantly suppressed for a molecular system with a phase relaxation originating in nuclear vibrations than for an atomic system with only a cavity relaxation.

On the basis of our present results, attractive effects of quantized fields such as squeezed fields on atomic systems are also expected on the coherency dynamics of molecular electronic systems though molecular vibrational effects, which tend to destroy the electronic coherency, strongly affect the dynamical behavior of off-diagonal molecular density matrices particularly. This suggests a possibility of direct control of molecular electronic coherency by a reflection of various quantum statistics of quantized photon fields.

We should finally mention the possibility of experimental observation of the present results. Unfortunately, the present model, i.e., two-level atom/molecule coupled with a single-mode strongly squeezed coherent light, is hard to be realized in experiments at the present time. However, the model with the same mathematical structure, i.e., the Jaynes-Cummings model, has been realized using the laser cooled trapped ions by the Wineland group [58–60]. They have created various nonclassical states, e.g., thermal, Fock, coherent, and squeezed states, of motion of a harmonically bound ^{9}Be$^+$ ion, and have measured the collapse-revival behaviors caused by the Jaynes-Cummings-type interaction between its motional and internal states, i.e., two hyperfine ground states, due to applied (classical) radiation [58]. They have also realized a decoherence induced by coupling the atom to controllable engineered reservoirs, i.e., amplitude and phase reservoirs, and have measured the decoherence of superposed motional states, i.e., Schrödinger cat states, of a single trapped atom [59,60]. These experiments using trapped ions are useful for the detailed comparisons between theory and experiment and the profound understanding of the relation among quantum phase dynamics and relaxations in the Jaynes-Cummings models involving the coupling with reservoirs. Judging from these results, the relaxation effects on the ringing revivals and the coherency between states obtained in this study have the sufficient possibility of being realized using the trapped ions with engineered reservoirs. Although in the present model the generation and decoherence of quantum superposed state appear in the photon phase dynamics with two mutually antirotating Q function distributions, i.e., "optical Schrödinger cat," such behavior is usually observed in mesoscopic systems because the macroscopic superposition decay so quickly [59,60]. Considering the large number of degrees of freedom in the mesoscopic systems, the present second-order MCWF approach is expected to be an effective

method for investigating the features of Schrödinger cat states, e.g., size and distribution dependency of its generation and collapse, in the mesoscopic systems coupled with reservoirs.

[1] E. T. Jaynes and F. W. Cummings, Proc. IEEE **51**, 100 (1963).

[2] L. Allen and J. H. Eberly, *Optical Resonance and Two-Level Atoms* (Wiley, New York, 1975).

[3] P. L. Knight and P. W. Milonni, Phys. Rep. **66**, 21 (1980).

[4] P. W. Milonni and S. Singh, Adv. At., Mol., Opt. Phys. **28**, 75 (1990).

[5] B. W. Shore and P. L. Knight, J. Mod. Opt. **40**, 1195 (1993).

[6] J. H. Eberly, N. B. Narozhny, and J. J. Sanchez-Mondragon, Phys. Rev. Lett. **44**, 1323 (1980).

[7] N. B. Narozhny, J. J. Sanchez-Mondragon, and J. H. Eberly, Phys. Rev. A **23**, 236 (1981).

[8] P. L. Knight and P. M. Radmore, Phys. Rev. A **26**, 676 (1982).

[9] F. T. Hioe, J. Math. Phys. **23**, 2430 (1982).

[10] R. R. Puri and G. S. Agarwal, Phys. Rev. A **33**, 3610 (1986).

[11] I. Sh. Averbukh, Phys. Rev. A **46**, R2205 (1992).

[12] P. F. Góra and C. Jedrzejek, Phys. Rev. A **48**, 3291 (1993).

[13] P. F. Góra and C. Jedrzejek, Phys. Rev. A **49**, 3046 (1994).

[14] P. F. Góra and C. Jedrzejek, Phys. Rev. A **45**, 6816 (1992).

[15] J. Gea-Banacloche, Phys. Rev. A **47**, 2221 (1993).

[16] A. Joshi and S. V. Lawande, J. Mod. Opt. **38**, 1407 (1991).

[17] T. M. Makhviladze and L. A. Shelepin, Phys. Rev. A **9**, 538 (1974).

[18] N. N. BogolubovJr., Fan Le Lien, and S. Shumovski, Phys. Lett. **101A**, 201 (1984).

[19] D. Meshede, H. Walther, and G. Müller, Phys. Rev. Lett. **54**, 551 (1985); G. Rempe, H. Walther, and N. Klein, *ibid.* **58**, 353 (1987); G. Rempe, F. Schmidt-Kaler, and H. Walther, *ibid.* **64**, 2783 (1990).

[20] M. Venkata Satyanarayana, P. Rice, Reeta Vyas, and H. J. Carmichael, J. Opt. Soc. Am. B **6**, 228 (1989).

[21] J. Eiselt and H. Risken, Phys. Rev. A **43**, 346 (1991).

[22] M. J. Werner and H. Risken, Phys. Rev. A **44**, 4623 (1991).

[23] S. Sachdev, Phys. Rev. A **29**, 2627 (1984).

[24] S. M. Barnett and P. L. Knight, Phys. Rev. A **33**, 2444 (1986).

[25] R. R. Puri and G. S. Agarwal, Phys. Rev. A **33**, 3610 (1986).

[26] Le-Man Kuang, Xin Chen, Guang-Hong Chen, and Mo-Lin Ge, Phys. Rev. A **56**, 3139 (1997).

[27] Ruixue Xu, YiJing Yan, and Xin-Qi Li, Phys. Rev. A **65**, 023807 (2002).

[28] M. Nakano, R. Kishi, T. Nitta, and K. Yamaguchi, J. Chem. Phys. **119**, 12106 (2003).

[29] D. Stoler, Phys. Rev. D **1**, 3217 (1970); **4**, 1925 (1971).

[30] H. P. Yuen, Phys. Rev. A **13**, 2226 (1976).

[31] D. W. Walls, Nature (London) **306**, 141 (1983).

[32] G. Milburn, Opt. Acta **31**, 671 (1984).

[33] M. V. Satyanarayana, P. Rice, R. Vyas, and H. J. Carmichael, J. Opt. Soc. Am. B **6**, 228 (1989).

[34] M. Nakano and K. Yamaguchi, Chem. Phys. Lett. **304**, 241 (1999).

[35] M. Nakano and K. Yamaguchi, J. Phys. Chem. A **103**, 6036 (1999).

[36] G. Milburn, Opt. Acta **31**, 671 (1984).

[37] W. H. Louisell, *Quantum Statistical Properties of Radiation* (Wiley, New York, 1973).

[38] J. Dalibard, Y. Castin, and K. Mølmer, Phys. Rev. Lett. **68**, 580 (1992).

[39] H. J. Carmichael, An Open Systems Approach to Quantum Optics, lectures presented at l'Université Libre de Bruxelles, Bruxells, Belgium, 1991, (unpublished).

[40] R. Dum, P. Zoller and H. Ritsch, Phys. Rev. A **45**, 4879 (1992).

[41] K. Mølmer, Y. Castin, and J. Dalibard, J. Opt. Soc. Am. B **10**, 524 (1993).

[42] M. B. Plenio and P. L. Knight, Rev. Mod. Phys. **70**, 101 (1998).

[43] J. Steinbach, B. M. Garraway, and P. L. Knight, Phys. Rev. A **51**, 3302 (1995).

[44] M. Nakano and K. Yamaguchi, Chem. Phys. Lett. **295**, 317 (1998).

[45] M. Nakano and K. Yamaguchi, Chem. Phys. **252**, 115 (2000).

[46] M. Nakano and K. Yamaguchi, Chem. Phys. Lett. **304**, 241 (1999).

[47] M. Nakano and K. Yamaguchi, J. Chem. Phys. **112**, 2769 (2000).

[48] M. Nakano and K. Yamaguchi, Chem. Phys. Lett. **324**, 289 (2000).

[49] M. Nakano and K. Yamaguchi, Chem. Phys. Lett. **317**, 103 (2000).

[50] M. Nakano and K. Yamaguchi, Phys. Rev. A **64**, 033415 (2001).

[51] M. Nakano and K. Yamaguchi, J. Chem. Phys. **116**, 10 069 (2002).

[52] M. Nakano and K. Yamaguchi, J. Chem. Phys. **117**, 9671 (2002).

[53] M. Nakano and K. Yamaguchi, Chem. Phys. **286**, 257 (2003).

[54] J. A. Wheeler, Lett. Math. Phys. **10**, 201 (1985).

[55] G. Lindblad, Commun. Math. Phys. **48**, 119 (1976).

[56] M. Nakano and K. Yamaguchi, Int. J. Quantum Chem. **95**, 461 (2003).

[57] H. J. Carmichael, *Statistical Methods in Qunatum Optics 1. Master Equations and Fokker-Planck Equations* (Springer, Berlin, 1999).

[58] D. M. Meekhof, C. Monroe, B. E. King, W. M. Itano, and D. J. Wineland, Phys. Rev. Lett. **76**, 1796 (1996).

[59] C. J. Myatt, B. E. King, Q. A. Turchette, C. A. Sackett, D. Kielpinski, W. M. Itano, C. Monroe, and D. J. Wineland, Nature (London) **403**, 269 (2000).

[60] Q. A. Turchette, C. J. Myatt, B. E. King, C. A. Sackett, D. Kielpinski, W. M. Itano, C. Monroe, and D. J. Wineland, Phys. Rev. A **62**, 053807 (2000).